

2019

Solidification cracking susceptibility of ferritic stainless steels using Modified Vareststraint Transvareststraint (MVT) method

D Konadu

University of Pretoria, University of Ghana

Pieter Georg Hendrik Pistorius

University of Pretoria

Madeleine Du Toit

University of Wollongong, mdt@uow.edu.au

Axel Griesche

Federal Institute for Materials Research and Testing

Follow this and additional works at: <https://ro.uow.edu.au/eispapers1>



Part of the [Engineering Commons](#), and the [Science and Technology Studies Commons](#)

Recommended Citation

Konadu, D; Pistorius, Pieter Georg Hendrik; Du Toit, Madeleine; and Griesche, Axel, "Solidification cracking susceptibility of ferritic stainless steels using Modified Vareststraint Transvareststraint (MVT) method" (2019). *Faculty of Engineering and Information Sciences - Papers: Part B*. 3125.
<https://ro.uow.edu.au/eispapers1/3125>

Solidification cracking susceptibility of ferritic stainless steels using Modified Varestraint Transvarestraint (MVT) method

Abstract

The Modified Varestraint Transvarestraint (MVT) test was used to investigate the solidification cracking susceptibility of an unstabilised, a Nb-stabilised and two (Ti + Nb) dual-stabilised ferritic stainless steels. Two different welding speeds of 6 and 3 mm/s using autogenous gas tungsten arc welding were employed. At the welding speed of 6 mm/s, the high-content (Ti + Nb) steel was resistant and the Nb-stabilised steel was marginally susceptible to solidification cracking. At the welding speed of 3 mm/s, the Nb and the high (Ti + Nb) steels were found to be marginally susceptible to solidification cracking while the unstabilised and low-content (Ti + Nb) grades were resistant to solidification cracking. The weld metal microstructures transverse to the welding direction revealed columnar grains in all the samples for both welding speeds. The ferritic stainless steels were generally resistant to solidification cracking, except the Nb-stabilised steel, which was marginally susceptible to solidification cracking.

Disciplines

Engineering | Science and Technology Studies

Publication Details

Konadu, D. S., Pistorius, P. G. H., Du Toit, M. & Griesche, A. (2019). Solidification cracking susceptibility of ferritic stainless steels using Modified Varestraint Transvarestraint (MVT) method. *Sadhana: academy proceedings in engineering sciences*, 44 (9), 194-1-194-6.



Solidification cracking susceptibility of ferritic stainless steels using Modified Vareststraint Transvareststraint (MVT) method

D S KONADU^{1,2,*}, P G H PISTORIUS¹, M DU TOIT³ and AXEL GRIESCHE⁴

¹Department of Materials Science and Metallurgical Engineering, University of Pretoria, Pretoria 0002, South Africa

²Department of Materials Science and Engineering, University of Ghana, P. O. Box LG 77, Accra, Ghana

³School of Mechanical, Materials, Mechatronic and Biomedical Engineering, University of Wollongong, Wollongong, Australia

⁴Bundesanstalt für Materialforschung und -prüfung (BAM), Federal Institute for Materials Research and Testing, Berlin, Germany
e-mail: dskonadu@ug.edu.gh

MS received 28 December 2018; revised 29 April 2019; accepted 2 July 2019

Abstract. The Modified Vareststraint Transvareststraint (MVT) test was used to investigate the solidification cracking susceptibility of an unstabilised, a Nb-stabilised and two (Ti + Nb) dual-stabilised ferritic stainless steels. Two different welding speeds of 6 and 3 mm/s using autogenous gas tungsten arc welding were employed. At the welding speed of 6 mm/s, the high-content (Ti + Nb) steel was resistant and the Nb-stabilised steel was marginally susceptible to solidification cracking. At the welding speed of 3 mm/s, the Nb and the high (Ti + Nb) steels were found to be marginally susceptible to solidification cracking while the unstabilised and low-content (Ti + Nb) grades were resistant to solidification cracking. The weld metal microstructures transverse to the welding direction revealed columnar grains in all the samples for both welding speeds. The ferritic stainless steels were generally resistant to solidification cracking, except the Nb-stabilised steel, which was marginally susceptible to solidification cracking.

Keywords. Modified Vareststraint Transvareststraint; solidification cracking; ferritic stainless steel; microstructure; welding; susceptibility.

1. Introduction

One of the defects potentially associated with welding is solidification cracking [1–3]. The combined effects of liquid film formation at grain boundaries, segregation of alloying elements and imposed thermo-mechanical strains can lead to solidification cracking during weld solidification. The presence of low-melting-point eutectic phases between the dendrites increases the risk of solidification cracking. Solidification cracking mostly occurs at the centreline of the weld [1, 4, 5]. For the measurement of solidification cracking susceptibility, different methods have been designed, which mainly comprise self-stressing samples or the application of external loads [4, 6–8]. The Vareststraint test is one of the most used tests based on the application of an external load. In this method, the specimen is bent with a defined bending rate around a die as the weld is being made [1, 4, 7, 9, 10]. In the Modified Vareststraint Transvareststraint (MVT) test, gas tungsten arc welding is used to re-melt the machined surface of a

sample. When the arc is at the centre of the specimen, a die with a defined radius is used to bend the specimen. The specimen thickness and the die radius produce different bending strains [4, 11, 12]. Standardised three given strain levels that are applied are $0\% > \epsilon_{cr} > 1\%$, $1\% > \epsilon_{cr} > 2\%$ and $2\% > \epsilon_{cr} > 4\%$, where ϵ_{cr} is the critical bending strain [12]. The surface of the weld metal is examined for the presence of cracks. If cracks are present, the total crack length is regarded as a quantitative measure of the susceptibility to solidification cracking.

Ferritic stainless steels find applications in chemical plants, pulp and paper mills, refineries, automobile trim, catalytic converters and decorative purposes [5]. Welding of ferritic stainless steels reduces toughness, ductility and corrosion resistance because of grain coarsening in the weld metal and in the heat-affected zone (HAZ) [4, 13–15]. Investigations of solidification cracking of stainless steels have been largely limited to duplex and austenitic stainless steels [16–18]. The addition of Ti and Nb has been said to decrease the resistance to solidification cracking in ferritic stainless steels [5]. In this project, an unstabilised, one mono-stabilised and two dual-stabilised ferritic stainless

*For correspondence
Published online: 19 August 2019

steels were tested for resistance to solidification cracking using the MVT test.

2. Experimental procedure

Four different alloys of an unstabilised (A:0Ti;0Nb), Nb-stabilised (B:0.6Nb), low Ti and Nb content (C:0.1Ti;0.4Nb) and high Ti and Nb content (D:0.4Ti;0.9Nb) dual-stabilised ferritic stainless steels were used for the experiment. Steels A:0Ti;0Nb and C:0.1Ti;0.4Nb were of commercial grades and steels B:0.6Nb and D:0.4Ti;0.9Nb were of experimental grades. Table 1 presents the chemical composition of the four ferritic stainless steels. Testing in the Varestraint mode to the DIN EN ISO 17641-3:2005 (E) standard was performed in BAM, the Federal Institute for Materials Research and Testing, Germany. The graph of total crack length against strain is divided into three sectors or regions, consistent with DIN EN ISO 17641-3:2005, with sector 1 being hot crack-resistant, sector 2 showing increasing hot crack susceptibility and sector 3 being prone to hot cracking. The borders of these sectors were developed based on a large body of experimental work by BAM, combined with practical knowledge [19]. The samples, with dimensions of 100 mm × 40 mm × 10 mm, were prepared by grinding and polishing the surface to a 1 µm finish. Dye penetration and ultrasonic testings were done before welding.

Autogenous gas tungsten arc welding at two different speeds of 6 and 3 mm/s were employed. Given the amount of available material, only one welding speed (6 mm/s) was used for the experimental steels B and D while all the steels were tested at welding speed of 3 mm/s. The 141 WIG-DC (DIN EN 287) welding process with a Cloos GLW 450 I-H-P-R power source and a shielding gas Argon 5.0-II (DIN EN ISO 14175) Air Liquide with flow rate 15 l/min was used. A 2.4 mm WC 20 (DIN EN 26848) electrode with an electrode tip of 30° was used. The samples were clamped and laid on mandrel dies of radii 125, 250 and 500 mm for 4%, 2% and 1% strain, respectively (figure 1). Heat input was calculated assuming a constant arc efficiency of 0.48 [3]. Ethyl alcohol was used to clean the polished surface before welding. Cracks were evaluated by treating the welded surface with Antox 71 E (etchant based on HNO₃ and HF) followed by stereoscopic microscopy at ×25

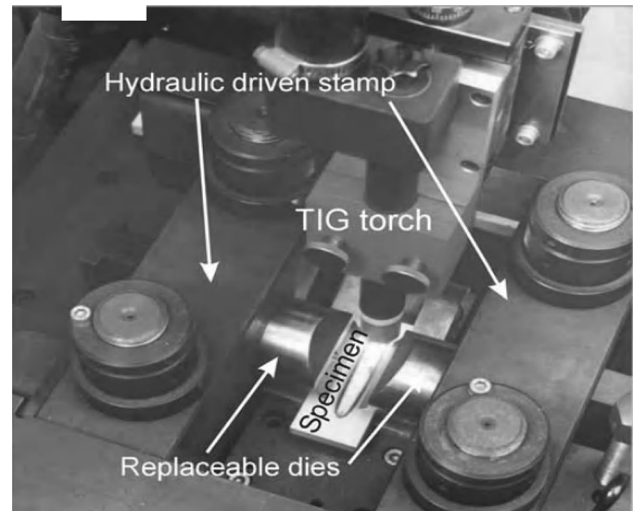


Figure 1. Example of the MVT test equipment [19].

magnification. The measurement of the crack length was executed in BAM, Germany, and also at the University of Pretoria (table 2). See figure 1 for an example of the experimental equipment [19]. The susceptibility to solidification cracking was quantified by plotting the total crack length against the strain rates. In addition to the MVT evaluation procedure, optical microscopy of a sectioning plane transverse to the welding direction was done. The sectioned surfaces were ground and polished to 1 µm finish. A solution comprising 1.5 g potassium disulphite, 5 ml HCl and 100 ml distilled water was used as an etchant [20]. For the microstructural analysis, an XM-15 optical microscope mounted with an Olympus U-TV0.5XC-3 camera with Stream Essentials software was employed.

3. Results

3.1 Stereoscope morphology

Not all the samples cracked (table 2 and figure 2). The observed cracks are solidification cracks because solidification cracks are often symmetrically formed (figure 2b) [19]. The total crack length measurements executed in the laboratories are compared. It was observed that the

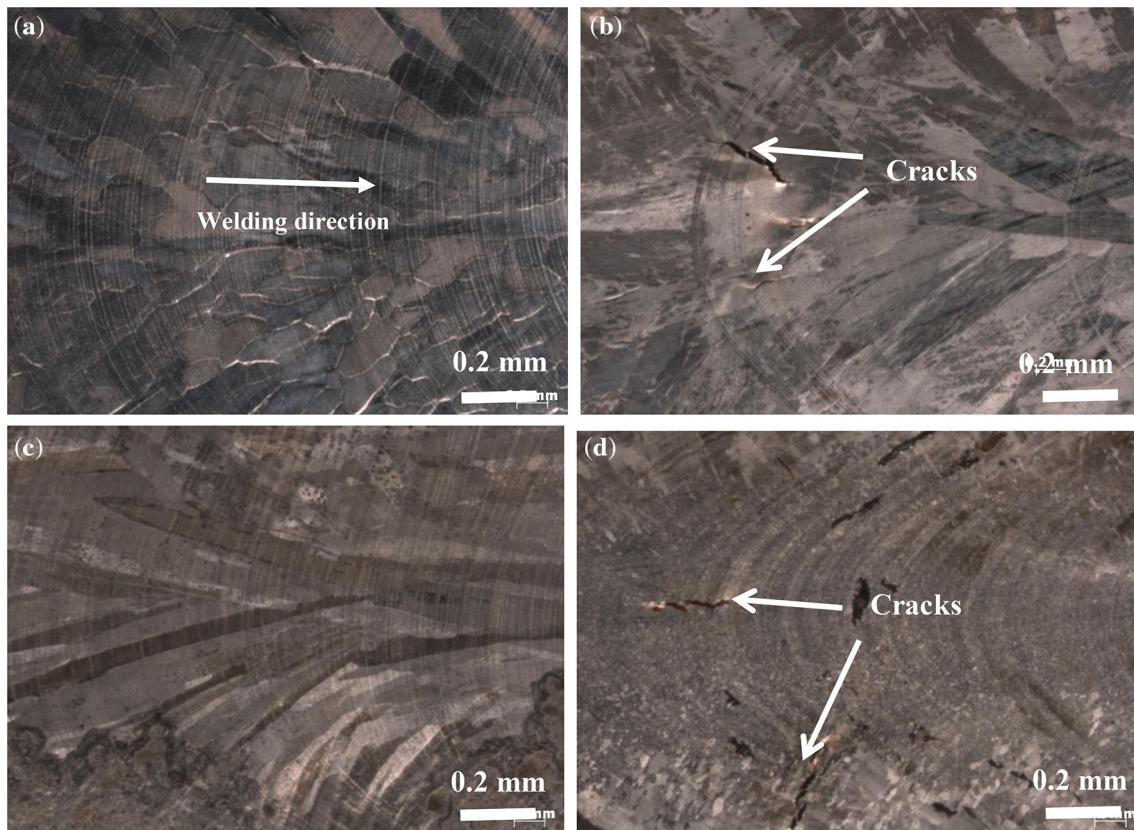
Table 1. The chemical composition of the ferritic stainless steels used for the study.

Element (wt%)	C	Si	Mn	P	S	N	Cr	Nb	Ti	Ni	Al
A:0Ti;0Nb	0.046	0.45	0.36	0.020	0.002	0.055	16.1	0.001	0.001	0.27	0.01
B:0.6Nb	0.012	0.42	0.33	0.024	0.007	0.07	18.8	0.58	0.03	0.23	0.03
C:0.1Ti;0.4Nb	0.011	0.49	0.43	0.025	0.002	0.015	17.5	0.396	0.11	0.15	0.01
D:0.4Ti;0.9Nb	0.011	0.44	0.37	0.025	0.004	0.067	18.2	0.92	0.36	0.37	0.02

Steel A and C were industrially produced, steel B and D were experimental grades.

Table 2. Welding parameters, strain and total crack length as measured after the Modified Vareststraint Transvareststraint test measurements from BAM and UP laboratories.

Steel	Current (A)	Voltage (V)	Heat input (kJ/mm)	Strain (%)	Welding speed (mm/s)	Total crack length (mm) BAM	Total crack length (mm) UP
(A:0Ti;0Nb)	219	12.3	0.43	1	3	0.0	0.0
(A:0Ti;0Nb)	218	13.1	0.46	2	3	0.0	0.0
(A:0Ti;0Nb)	218	12.1	0.42	4	3	0.0	0.0
(B:0.6Nb)	218	13.1	0.46	1	3	0.5	0.0
(B:0.6Nb)	219	13.6	0.48	2	3	0.7	0.2
(B:0.6Nb)	218	12.7	0.44	4	3	3.2	3.8
(C:0.1Ti;0.4Nb)	219	12.1	0.42	1	3	0.0	0.0
(C:0.1Ti;0.4Nb)	218	12.5	0.44	2	3	0.0	0.0
(C:0.1Ti;0.4Nb)	218	12.2	0.43	4	3	0.0	0.0
(D:0.4Ti;0.9Nb)	218	12.6	0.44	1	3	2.9	1.9
(D:0.4Ti;0.9Nb)	219	13.1	0.46	2	3	1.6	0.7
(D:0.4Ti;0.9Nb)	218	12.4	0.43	4	3	11.0	11.7
(B:0.6Nb)	256	13.8	0.28	1	6	1.2	1.7
(B:0.6Nb)	256	14.4	0.29	2	6	2.6	2.8
(B:0.6Nb)	256	14.0	0.29	4	6	6.6	10.1
(D:0.4Ti;0.9Nb)	256	13.4	0.27	1	6	0.0	0.0
(D:0.4Ti;0.9Nb)	256	14.1	0.29	2	6	1.2	0.0
(D:0.4Ti;0.9Nb)	256	13.5	0.28	4	6	6.6	7.8

**Figure 2.** Typical stereoscopic images showing (a) alloy A:0Ti;0Nb with no crack at a welding speed of 3 mm/s and strain 1%, (b) solidification cracks in the B:0.6Nb-stabilised ferritic stainless steel at a welding speed of 6 mm/s and 2% strain, (c) alloy C:0.1Ti;0.4Nb with no crack at a welding speed of 3 mm/s and 1% strain and (d) solidification cracks in alloy D:0.4Ti;0.9Nb at a welding speed of 6 mm/s and 2% strain ($\times 25$). For all four images, the welding direction was as shown.

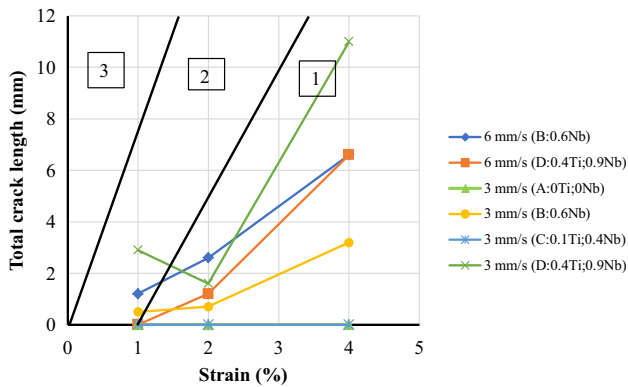


Figure 3. Total crack length vs strain for the welding speeds of 6 and 3 mm/s (BAM). Region 1: hot crack resistant, Region 2: increasing hot cracking susceptibility, Region 3: hot crack-prone. Every data point represents the total crack length on one sample.

measurements of University of Pretoria (UP) were higher by about 15% on average. Overall, the UP measurements were in agreement with the BAM total crack length measurements as all the cracks were located in the same sectors for both sets of measurements. The measurements by the two laboratories indicated that there was no significant difference in the susceptibility to solidification cracking for a steel grade for a specific combination of welding speed and strain rate. The total crack length, as determined using the BAM measurements, is plotted in figure 3.

3.2 Susceptibility to solidification cracking, as quantified by the total crack length

The total crack length increased with increasing strain for all the experimental steels, consistent with published behaviour [21], except the experimental D:0.4Ti;0.9Nb alloy, where the total crack length initially decreased and then increased with increasing strain (table 2 and figure 3). For the commercial steels, there were no cracks; as indicated by the symbols for alloys A and D, on the x-axis (figure 3). All the measured cracks were classified to be in the hot crack resistance sector (sector 1 in figure 3) with two exceptions:

- The first exception was the experimental 0.6Nb-stabilised ferritic stainless steel (B:0.6Nb) at a strain of 1%, which was in sector 2 and at welding speeds of 6 and 3 mm/s, indicating that this grade was marginally susceptible to solidification cracking at both welding speeds.
- The second exception was the D:0.4Ti;0.9Nb steel at 1% strain for a welding speed of 3 mm/s, indicating that steel D:0.4Ti;0.9Nb was also marginally crack sensitive.

The two commercial steels (steel A:0Ti;0Nb and steel C:0.1Ti;0.4Nb) did not crack at any strain. From figure 3

and table 2, it is seen that increasing welding speed increases the total crack length for B:0.6Nb ferritic stainless steel. The reverse was observed in the D:0.4Ti;0.9Nb grade, in that, decreasing the welding speed from 6 to 3 mm/s showed an increase in total crack length. The behaviour of the D:0.4Ti;0.9Nb grade was inconsistent in that the crack length at 3 mm/s was higher than that at 6 mm/s. It is also seen from figure 3 without the sectors that D:0.4Ti;0.9Nb at a welding speed of 3 mm/s had the greatest sensitivity to solidification cracking. B:0.6Nb at both welding speeds (6 and 3 mm/s) and D:0.4Ti;0.9Nb at a welding speed of 6 mm/s showed intermediate sensitivity to solidification cracking. C:0.1Ti;0.4Nb and A:0Ti;0Nb were the least sensitive to solidification cracking [22].

3.3 Microstructure surrounding the solidification crack

The optical microstructure of the plane transverse to the welding direction revealed mostly columnar grains. There were sub-surface cracks that were not visible as solidification cracks on the upper surface of the sample. The orientation of the micrograph with respect to the fusion line is presented in figures 4–6. Figures 4–6 show columnar grains and the sub-surface cracks for the D:0.4Ti;0.9Nb grade are revealed in figure 6. Figure 4 shows the microstructure of the commercial unstabilised steel as having a little sawtooth martensite located at the ferrite grain boundaries. Table 3 summarises the solidification structure of the microstructures transverse to the welding direction. At a welding speed of 3 mm/s, the weld metal structure was equiaxed – columnar (steel A), or columnar (steel B, steel C and steel D). At a welding speed of 6 mm/s, the weld metal structure was columnar (steel B and steel D).

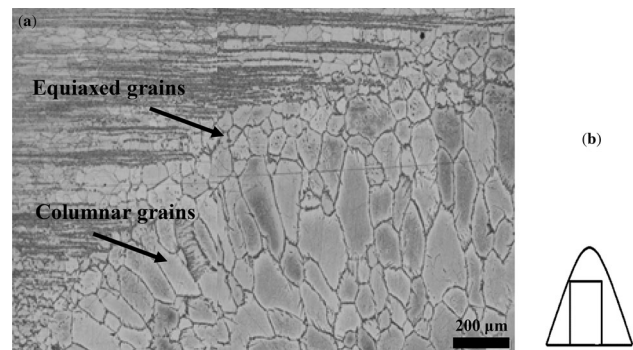


Figure 4. Microstructure of the unstabilised ferritic stainless steel (A:0Ti;0Nb) at 2% strain and welding speed of 3 mm/s showing (a) the base metal, HAZ region and the weld centre and (b) schematic orientation of the micrographs with respect to the fusion zone.

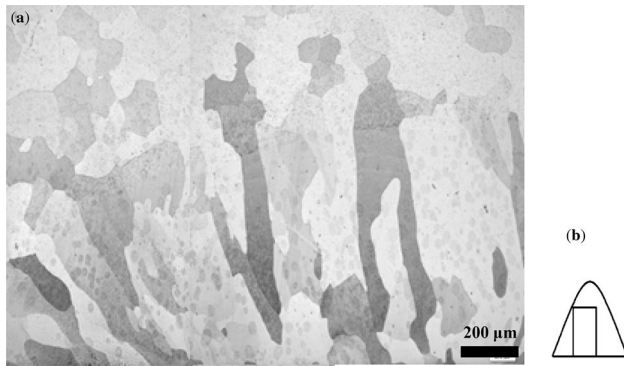


Figure 5. Microstructure of the 0.6Nb-stabilised ferritic stainless steel (B:0.6Nb) at 2% strain and welding speed of 6 mm/s showing (a) the base metal, HAZ region and the weld centre and (b) schematic orientation of the micrographs with respect to the fusion.

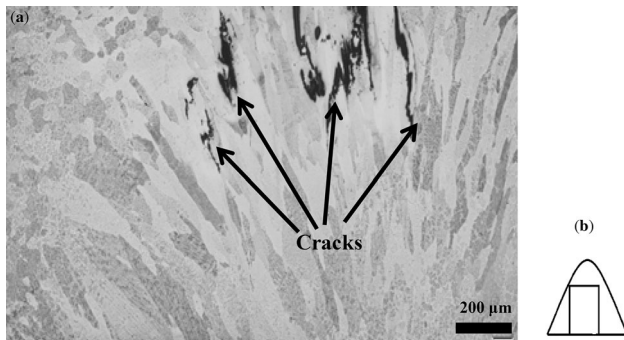


Figure 6. Microstructure of the 0.4Ti + 0.9Nb-stabilised ferritic stainless steel (D:0.4Ti;0.9Nb) at 4% strain showing (a) the base metal, HAZ region and the weld centre at a welding speed of 3 mm/s and (b) schematic orientation of the micrographs with respect to the fusion.

Table 3. The solidification structure of the weld metal, as observed on a polished plane transverse to the direction of the weld.

Steel grade	Welding speed (mm/s)	Solidification structure
A:0Ti;0Nb	3	Equiaxed grains close to the fusion line; columnar grains at the centreline of the weld (figure 4)
B:0.6Nb	3	Columnar
B:0.6Nb	6	Columnar (figure 5)
C:0.1Ti;0.4Nb	3	Columnar
D:0.4Ti;0.9Nb	3	Columnar (figure 6)
D:0.4Ti;0.9Nb	6	Columnar

4. Discussion

The total crack length as measured at two laboratories differed by, on average, about, generally, 15%. Despite this difference, the evaluation of the susceptibility to solidification cracking yielded similar results for different ferritic stainless steels.

Generally, Nb increases the risk of solidification cracking in steels [4]. The commercial unstabilised ferritic stainless steel (steel A) was found to be resistant to the solidification cracking. The zero Ti and Nb content might have eliminated the low-melting-point eutectic phases associated with Ti and Nb in ferritic stainless steels [5]. The commercial unstabilised A:0Ti;0Nb was seen to have a little sawtooth martensite, which was located at the ferrite grain boundary. The commercial unstabilised A:0Ti;0Nb steel has a 0.046 wt% C (which is slightly higher than average (table 1)) and some austenite might have formed along the ferrite grain boundaries. The austenite then transformed to martensite when the weld metal cooled to room temperature. This agrees with Lippold and Kotecki [5] as it is reported that 0.05 wt% carbon does form martensite at the ferrite grain boundary.

The 0.6Nb-stabilised ferritic stainless steel (B:0.6Nb) at strain 1, which was in sector 2, indicated that this grade was marginally susceptible to solidification cracking at the welding speeds 6 and 3 mm/s. This could be attributed to the Nb content (0.6% Nb), which has been found to form a eutectic at 1373 °C with Fe [4, 23]. The presence of this eutectic increases the brittle temperature range. Moreover, Nb has also been seen to be detrimental to steels by promoting solidification cracking through columnar grain formation [4].

The commercial dual-stabilised steel (C:0.1Ti;0.4Nb) was found to be resistant to solidification cracking. This could be due to the low Ti + Nb contents, which were not high enough to increase the brittle temperature range or to form low-melting eutectic phases associated with Ti and Nb stabilisation in ferritic stainless steels [5]. They might have contributed to the solidification crack resistance. The D:0.4Ti;0.9Nb grade was also marginally crack sensitive at welding speed 3 mm/s. This could be due to the high Ti + Nb contents in the steel [5]. The behaviour of steel D:0.4Ti;0.9Nb was considered to be inconsistent, with a longer crack at a welding speed of 3 mm/s than at 6 mm/s, at 4% strain (table 2); the longer crack was expected at a higher welding speed. Furthermore, for the same alloy composition, at a welding speed of 3 mm/s, an increase in strain from 1% to 2% resulted in an unexpected decrease in total crack length (table 2). Moreover, it was found that the same alloy was marginally susceptible at a welding of 3 mm/s and resistant to solidification cracking at a welding speed of 6 mm/s. Higher welding speeds are known to be susceptible to solidification cracking but it was rather the lower welding speed of 3 mm/s which was marginally susceptible.

Teardrop pool shapes are found at high welding speeds, which result in columnar grains [1, 2]. The two welding speeds were considered to be high and this produced the columnar grains in all the steels welded at 6 and 3 mm/s. The mechanism for solidification cracking was likely to be that eutectic components (containing Ti and Nb) increased the brittle temperature range.

5. Conclusions

1. The unstabilised and the low-content dual-stabilised ferritic stainless steels were crack resistant at all welding speeds.
2. The Nb-containing ferritic stainless steel (B:0.6Nb) was marginally susceptible to solidification cracking at both welding speeds of 3 and 6 mm/s. The (D:0.4Ti;0.9Nb) steel was resistant to solidification cracking at a welding speed of 6 mm/s. The same alloy showed marginal resistance to solidification cracking at a welding speed of 3 mm/s.
3. The solidification structure of the weld metal was dominated by columnar grains at all welding speeds.

Acknowledgements

The authors want to thank Office of Research, Innovation, and Development (ORID), University of Ghana, Department of Research and Innovation Support (DRIS), University of Pretoria and the Southern African Institute of Welding (SAIW) for financial assistance. The authors are also grateful to BAM, the Federal Institute for Materials Research and Testing, Germany, for the execution of the experiment.

References

- [1] Kou S (Ed) 2003 *Welding Metallurgy*. Hoboken: Wiley
- [2] Lippold J C 2015 *Welding Metallurgy and Weldability*. Hoboken: Wiley
- [3] Lancaster J F (Ed) 1999 *Metallurgy of Welding*. Abington: Woodhead Publishing Limited
- [4] Folkhard E 1988 *Welding Metallurgy of Stainless Steels*. Vienna: Springer
- [5] Lippold J C and Kotecki D J 2005 *Welding Metallurgy and Weldability of Stainless Steels*. Hoboken: Wiley
- [6] Campbell R D and Walsh D W 1993 Weldability testing. In: Hugh Baker (ed) *ASM Handbook*, vol. 6. ASM International, United States of America
- [7] Lundin C D, DeLong W T and Spond D F 1976 The fissure bend test. *Weld. J.* 55 (Res. Suppl.): 145–151
- [8] Srinivasan G, Divya M, Das C R, Albert S K, Bhaduri A K, Lauf S, Stubenrauch S and Klenk A 2015 Weldability studies on borated stainless steel using Varestraint and Gleeble test. *Weld. World* 59: 119–126
- [9] Savage W F and Lundin G D 1965 The Varestraint test. *Weld. J.* 44: 433–442
- [10] Nelson D E, Baeslack III W A and Lippold J C 1987 An investigation of weld hot cracking in duplex stainless steels. *Weld. J.* 66: 241s–250s
- [11] Thomas B, Herold H, Cross C E and Lippold J C 2008 *Hot Cracking Phenomena in Welds II*. Berlin: Springer
- [12] Kannengiesser T and Boellinghaus T 2014 Hot cracking tests—an overview of present technologies and applications. *Weld. World*. 57(1): 3–37
- [13] Mohandas T, Madhusudhan R G and Naveed M 1999 A comparative evaluation of gas tungsten and shielded metal arc welds of a ferritic stainless steel. *J. Mater. Process. Technol.* 94(2–3): 133–140
- [14] Parmar R S 2003 *Welding Processes and Technology*. New Delhi: Khanna Publishers
- [15] Silva C C, Farias J P, Miranda H C, Guimarães R F, Menezes J W A and Neto M A M 2008 Microstructural characterization of the HAZ in AISI 444 ferritic stainless steel welds. *Mater. Charact.* 59(5): 528–533
- [16] Shankar V, Gill T P, Mannan S and Sundaresan S 2003 Effect of nitrogen addition on microstructure and fusion zone cracking in Type 316L stainless steel weld metals. *Mater. Sci. Eng. A* 343(1–2): 170–181
- [17] Sun Z 1992 A study of solidification crack susceptibility using the solidification cycle hot-tension test. *Mater. Sci. Eng. A* 154: 85–92
- [18] Varol I, Baeslack III W A and Lippold J C 1989 Characterization of weld solidification cracking in a duplex stainless steel. *Metallography* 23: 1–19
- [19] Böllinghaus T and Herold H 2005 *Hot Cracking Phenomena in Welds*. Berlin: Springer
- [20] Vander Voort G F 2007 *Metallography Principles and Practices*. New York: ASM International
- [21] Ankara A and Ari H B 1997 Determination of hot crack susceptibility of various kinds of steels. *Mater. Des.* 17(5): 261–265
- [22] Savage W F and Lundin C D 1966 Application of the Varestraint technique to the study of weldability. *Weld. J.* 45(11): 496–s–503-s
- [23] Notis R M, Gjostein N A, Jessen Jr. N C and Kendall E C 1992 Alloy phase diagrams. In: Hugh Baker (ed) *ASM Handbook*, vol. 3. ASM International, United States of America